




Influence of fused deposition modelling printing parameters on tablet disintegration times: a design of experiments study

KLEMEN KREFT^{1,2} 
TIJANA STANIČ²
PETRA PERHAVEC²
ROK DREU¹ 
ZORAN LAVRIČ^{1,*} 

¹ University of Ljubljana, Faculty of Pharmacy, 1000 Ljubljana, Slovenia

² Lek Pharmaceuticals d.d., a Sandoz Company, 1000 Ljubljana, Slovenia

ABSTRACT

Despite the importance of process parameters in the printing of solid dosage forms using fused deposition modelling (FDM) technology, the field is still poorly explored. A design of experiment study was conducted to understand the complete set of process parameters of a custom developed FDM 3D printer and their influence on tablet disintegration time. Nine settings in the Simplify 3D printing process design software were evaluated with further experimental investigation conducted on the influence of infill percentage, infill pattern, nozzle diameter, and layer height. The percentage of infill was identified as the most impactful parameter, as increasing it parabolically affected the increase of disintegration time. Furthermore, a larger nozzle diameter prolonged tablet disintegration, since thicker extruded strands are generated through wider nozzles during the printing process. Three infill patterns were selected for in-depth analysis, demonstrating the clear importance of the geometry of the internal structure to resist mechanical stress during the disintegration test. Lastly, layer height did not influence the disintegration time. A statistical model with accurate fit ($R^2 = 0.928$) and predictability ($Q^2 = 0.847$) was created. In addition, only the infill pattern and layer height influenced both the uniformity of mass and uniformity of the disintegration time, which demonstrates the robustness of the printing process.

Keywords: 3D printed tablets, disintegration time, fused deposition modelling, design of experiments, printing parameters, uniformity of mass

Accepted April 25, 2023
Published online April 25, 2023

Fused deposition modelling in a pharmaceutical setting is a novel 3D printing technology to adopt personalised treatment in traditional medicine. Material screening (1–4), filament characteristics (5–7), release kinetics (8–10) and tablet shape (11–13) have already

* Correspondence; email: zoran.lavric@ffa.uni-lj.si

been extensively researched. On the other hand, process parameter investigation has not been widely addressed for pharmaceutical purposes. The reason might be the vast availability of different implementations of printing design and slicing software that also controls the printing process. Each printing design, slicer, and process control software has its own settings, meaning that process parameters can hardly be compared between different studies and drawing conclusions is misleading (14). Novel slicing software tools are devised with in-depth process parameters optimized for the printing process (15). This is an opportunity to standardise the printing parameters for pharmaceutical purposes. Additionally, each 3D printer has its own distinctive geometric and performance features, demonstrating that the values of the process parameters should be tailored to each machine (16, 17). For example, filament liquefiers differ from each other in size, accuracy, and capacity to process material (18). Therefore, the filament processing within the liquefier might be variable for each printer, and the temperature of the liquefier should be adjusted. The same applies to other parameters of the printing process.

Previous research has already addressed the dosage form design to some extent. Infill percentage demonstrated a clear influence on dissolution time of various API. Increase in the infill percentage results in longer release profiles due to a thicker, more compact core with lower porosity (8, 19–22). The infill patterns were also determined to have an impact (23). By improving the internal structure of the core *via* various patterns, the release profile can be extended. In case of MakerWare slicer software, the diamond infill pattern appears to yield the slowest release, while the linear or hexagonal pattern generates the fastest release (20, 21, 24, 25). However, many printing design and slicer software offer a predetermined set of patterns to choose from, which are different for each software implementation. Although important findings were published, it was not possible to relate the results between each study due to the specifics of the different slicers that were used. Furthermore, the influence of the layer height on the drug release profiles appears to be divisive. Theophylline release from Eudragit RL was somewhat reduced at the layer height of 0.4 mm compared to the layer heights of 0.1 and 0.2 mm (26). On the contrary, the caffeine release from a combination of polycaprolactone (PCL) and polyvinylpyrrolidone-vinyl acetate (PVP-VA) matrix was prolonged for the first 8 hours at the layer height of 0.2 mm, compared to 0.3 and 0.4 mm (21). Furthermore, a decrease in mechanical properties was reported for polylactic acid (PLA) printed objects when changing the layer height from 0.1 to 0.3 mm, which might indicate a faster drug release (27). Overall, the impact of layer height on drug release is not yet clear. The printing speed is also relevant, since a moderate printing speed (30–60 mm s⁻¹) leads to stronger and better quality prints. At higher speeds (> 75 mm s⁻¹), the printed layer is incompletely solidified and does not provide adequate support for the following layers, leading to a structure of poor quality. Slower speeds (< 15 mm s⁻¹) cause longer residence times in the hot nozzle, resulting in increased filament softening with the ensuing potential extrusion difficulties (23, 28). Additionally, a long residence time exposes the drug substance to more heat, which can result in drug degradation. In the case of carvedilol, mainly the slow printing speed of 10 mm s⁻¹ contributed to excessive total product impurities (6). Alhijaj *et al.* constructed a comprehensive review of several materials, printing equipment, and process parameters and their influence on the weight and dimensional accuracy of printed objects. Although API release was not the primary focus of the study, it offers a valuable insight into equipment and process variables (29).

Despite already published research, several process parameters were not yet explored. In addition, certain published findings are contradictory, for example, the influence of layer height. To understand the printing process and its influence on the final product, a preliminary study was first designed to explore 9 dosage form design and process parameters and their influence on the disintegration time of FDM printed tablets. Next, a design of experiment (DoE) study was created with careful selection of important parameters to understand the impact on disintegration time, uniformity of disintegration time, and uniformity of mass with the Simplify3D slicer software.

EXPERIMENTAL

Materials and 3D printing

Fast-soluble polyvinyl alcohol (PVA) filament of 1.75 mm thickness was purchased from eSUN (eSUN, China). Capsule-shaped tablets with dimensions of 18.0 × 8.0 mm with a fillet of 2 mm and without top and bottom layers were designed in SOLIDWORKS® 2018 (Dassault Systèmes, USA). The object volume designs were structured, sliced, and prepared for printing with Simplify3D® software (Simplify3D, USA). 3D printing was performed on a custom-made 3D printer FDM-3P (Zavod 404, Slovenia) (Fig. 1). It is composed of three printheads for simultaneous printing with three different filaments. Each printhead is equipped with two external ventilators to rapidly cool the deposited material. All printing was performed through the first printhead to prevent any potential variability between printheads. The printbed is large enough to accommodate up to 30 tablets in a single printing cycle. To improve tablet adhesion, the printbed was covered with 3M blue painter's

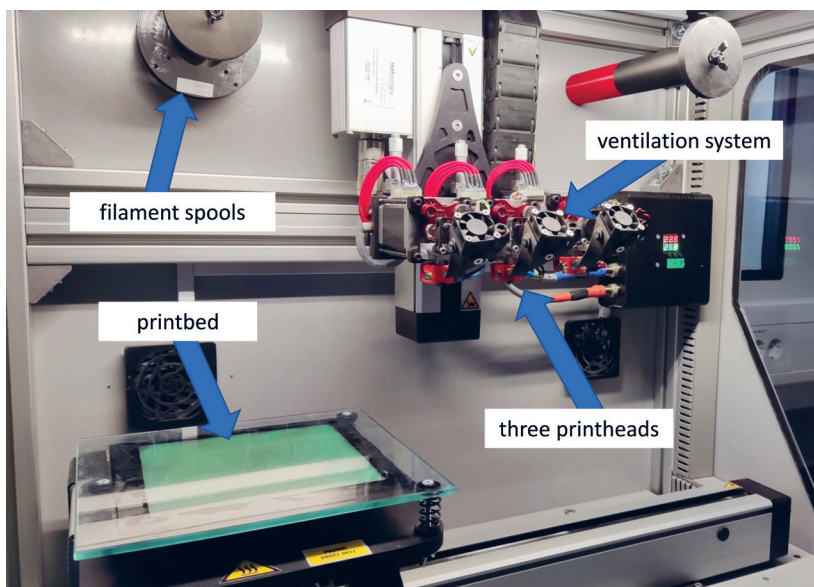


Fig. 1. FDM 3P 3D printer with main parts.

tape. The printing temperature was set to 165 °C to reach adequate filament flow from the printer nozzle, while the printbed was heated to 50 °C. If not explicitly specified, the following process parameters were set: 20 % infill, 0.2 mm layer height, rectilinear infill pattern, 50 % outline overlap, no top or bottom layers, and 0.3 mm nozzle diameter. The printer was operated at a speed of 20 mm s⁻¹. All tablets were rapidly cooled during printing *via* an air-cooling ventilation system to prevent dimension variation due to slow cooling. Six tablets were prepared for each specific experiment in the preliminary and the following DoE study. By varying the height of the tablet, the mass was maintained at approximately 300 ± 12 mg. The height of the tablet ranged from 4.2 to 7.6 mm.

Selection of process parameters in the preliminary study

The Simplify3D software was studied for suitable tablet design and printing parameters and 9 were explored: infill percentage, infill pattern, printing layer height, outline overlap, start point, presence of top and bottom layers, printing mode, presence of tablet shell and nozzle diameter:

- Infill percentage represents the extent of filling of the tablet core (0–100 %). Higher infill percentages can retard drug release and *vice versa* (Fig. 2a).
- The diameter of the nozzle represents the size of the printing nozzle. Thicker filament strands will flow through wider nozzles with potential effect on interlayer fusion and disintegration time (Fig. 2b).
- Layer height is the height of each extruded layer. At lower layer height, more layers will have to be printed to achieve the same tablet height. However, layers are flatter when lower layer height is selected, leading to increased interlayer contact and potential impact on disintegration time (Fig. 2c).
- The infill pattern is the geometry of the core filling. Six basic infill patterns (wiggle, triangular, rectilinear, grid, fast honeycomb, full honeycomb) are available with potential influence on the internal structure of the tablet and the surface area for polymer dissolution (Fig. 2d).
- The outline overlap represents the percentage of contact between the shell and infill. High outline overlap could improve internal tablet stability and increase disintegration times (Fig. 2e).
- The starting point setting controls the printing movement at the beginning of each layer and the printing time. At random starting points, each new layer starts printing at a different location, while the printing time is longer. The optimised starting points are aligned on the same axis, where each new layer starts printing at the same location on top of the previous layer. As a result, the printing time is shorter. In the latter case, depending on the alignment of the filament structures between layers, an excess of material deposition might occur on the same vertical or slanted axis along the printed tablet. This could create a series of strong points with better resistance against tablet disintegration, while the printing time is reduced (Fig. 2f).
- The printing mode describes how the tablets will be printed. Sequential mode prints each tablet entirely before moving on to the next. The continuous mode first prints each layer of each tablet and then moves to the next layer. In the case of sequential mode, the printed layers do not fully solidify before a new layer is deposited. This could result in greater interlayer fusion and increased disintegration time (Fig. 2g).

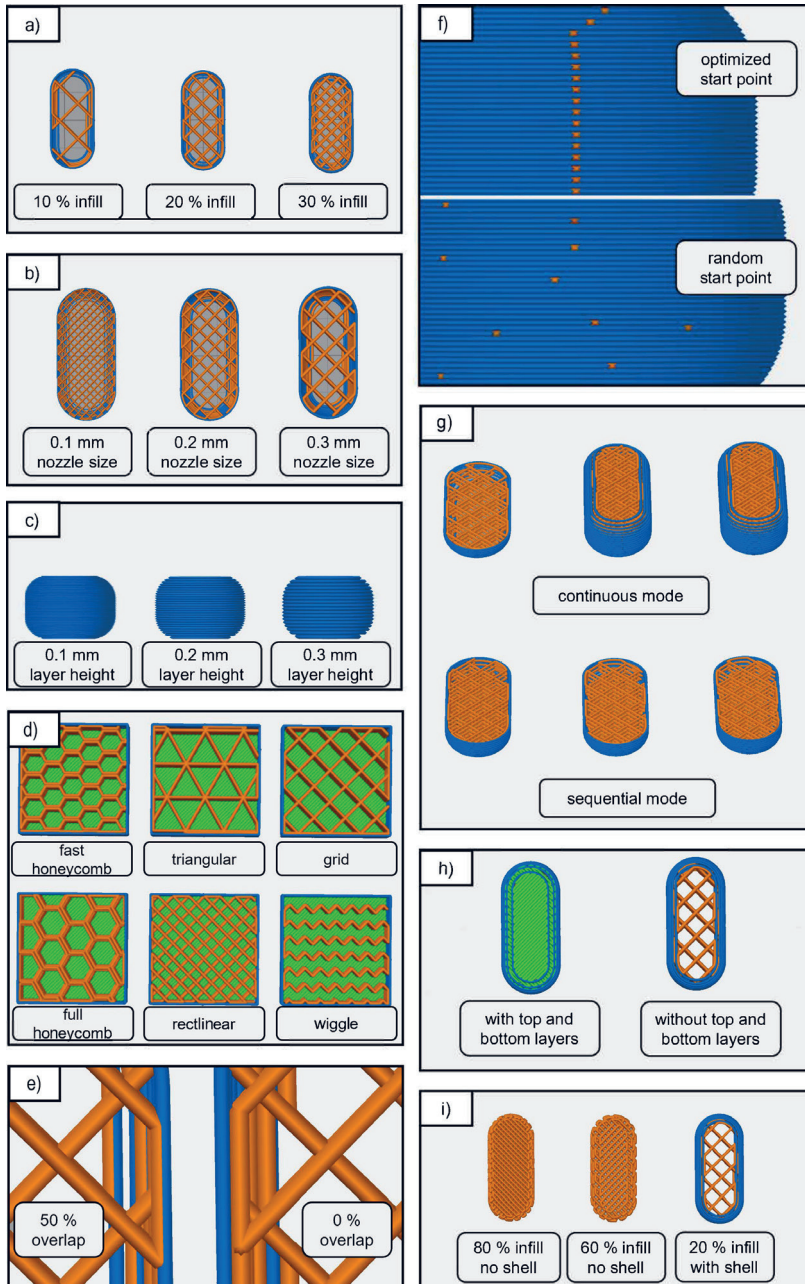


Fig. 2. Visualisation of printing parameters and display of settings in preliminary studies. a) Infill percentage; b) nozzle size; c) layer height; d) infill pattern; e) outline overlap; f) start point; g) printing mode; h) top and bottom layer presence and i) shell presence.

- The presence of solid top and bottom layers blocks water entry and increases the disintegration time (Fig. 2h).
- The shell defines the number of outline layers that surround the core of the tablet. The shell creates a barrier for water intrusion, while high infills without the shell form a resistant internal structure (Fig. 2i).

Design of experiment study

A DoE study was set up with statistical software Modde 12.01 (Sartorius, Germany) to conduct a thorough investigation of the relevant printing parameters in terms of disintegration time, mass uniformity and disintegration time uniformity. A D-optimal study design was selected with 28 experimental runs (Table I). Three levels were defined for each parameter. The infill was varied between 20, 30 and 40 %, the infill pattern between wiggly, rectilinear, and grid, the nozzle size between 0.2, 0.3 and 0.4 mm. The layer height was set to 33.3, 66.6 and 100 % of the nozzle size, since the layer thickness should not exceed the nozzle size for optimal printability.

Analysis of tablets

The prepared tablets or tablet-like structures were analysed for disintegration time, mass uniformity, and disintegration time uniformity. Tablet mass was determined on an analytical scale (Sartorius AX224, Sartorius AG, Germany) in 6 replicates and an average mass and relative standard deviation (RSD) were calculated. The disintegrating apparatus ERWEKA ZT4 (Erweka, Germany) was used to perform disintegration tests in 6 replicates according to TEST A of the European Pharmacopoeia (10th edition, 2020; 2.9.1. Disintegration of tablets and capsules) with distilled water at 37.0 °C used as immersion fluid. Due to the swelling nature and the potential sticking of the tablets, disks were not used in the study. Tablets were deemed disintegrated when no residue was visible within the tubes or the wire cloth.

RESULTS AND DISCUSSION

Preliminary study

Before designing and executing the DoE study, nine printing parameters were first screened to establish their influence and relations with the disintegration time. The percentage of infill, the pattern of infill, the height of the layer, and the diameter of the nozzle exhibited some influence on the disintegration time. However, the relationship was not clear at all levels. The percentage of infill can affect the dissolution and disintegration of 3D printed tablets. This was confirmed as 30 % infill resulted in a longer disintegration time; however it was similar for 10 and 20 % infills (Fig. 3a). Since the infill was very low, the core of the tablet quickly disintegrated in both cases. The remaining shell determined the final disintegration time. Since the shell mass was similar for 10 and 20 % infill, the disintegration time was also comparable. It appears that at 30 % infill and higher, its effect on the prolongation of disintegration time dominates compared to the shell. For the nozzle size, faster disintegration was observed when the 0.2 mm size was used, while the sizes of

0.3 and 0.4 mm lead to somewhat slower disintegration (Fig. 3b). In case of larger nozzles, thicker extruded strands are deposited on the printbed. A wider shell and more contact between layers are expected, leading to longer disintegration. The layer height demonstrated a less straightforward impact (Fig. 3c). The 0.1 mm layer height prolonged the disintegration time, while there was no difference between the 0.2 and 0.3 mm layer heights. Several infill patterns were also tested for their ability to advance the resistance of the

Table I. Process parameter settings for each DoE run

Run	Infill (%)	Infill pattern	Layer height (μm)	Nozzle size (mm)
N1	20	wiggle	132	0.4
N2	40	wiggle	200	0.2
N3	20	wiggle	133	0.2
N4	20	wiggle	300	0.3
N5	40	wiggle	266	0.4
N6	40	wiggle	99	0.3
N7	30	wiggle	66	0.2
N8	30	wiggle	400	0.4
N9	40	rectilinear	66	0.2
N10	20	rectilinear	200	0.2
N11	40	rectilinear	200	0.2
N12	20	rectilinear	400	0.4
N13	40	rectilinear	400	0.4
N14	20	rectilinear	99	0.3
N15	30	rectilinear	132	0.4
N16	20	grid	66	0.2
N17	40	grid	132	0.4
N18	20	grid	200	0.2
N19	40	grid	400	0.4
N20	20	grid	266	0.4
N21	40	grid	133	0.2
N22	30	grid	200	0.3
N23	30	grid	200	0.3
N24	30	grid	200	0.3
N25	30	grid	200	0.3
N26	30	rectilinear	200	0.3
N27	30	rectilinear	200	0.3
N28	30	rectilinear	200	0.3

tablet to disintegration at 30 % infill. The disintegration times were in increasing order as follows: wiggle < triangular < rectilinear < fast honeycomb < full honeycomb < grid (Fig. 3d). The pattern of the tablet core clearly demonstrated the influence on the tablet's ability to retain shape. The wiggle pattern resulted in the shortest disintegration with the least amount of internal support, as the tablet core quickly disintegrated. On the other hand, the grid pattern provided the longest disintegration time. A DoE study was designed to further assess these four printing parameters.

The starting point distribution, the continuous and sequential printing modes, and the outline overlap do not appear to have an impact on the disintegration time of tablets (Figs. 3e, 3f, and 3g). The axially aligned starting point setting optimised for printing time does not create an axis of strong points, but it significantly reduces the printing time compared to the random start point. In both cases, the disintegration time is comparable. Therefore, an optimised setting is the preferred option, as longer printing times can lead to greater drug degradation. A similar conclusion was reached for the printing mode. Continuous and sequential mode settings are comparable in disintegration time. Although continuous printing mode leads to a lower RSD in disintegration time, the printing process is slower and can include unnecessary oozing. Oozing can be explained as unwanted material deposition outside of the printing range. This can happen due to constant nozzle heating as filament can leak from the nozzle. When the print head is moving over an open space between objects, material deposition is not desired. To facilitate the printing process and reduce printing time, sequential printing mode is preferred. Outline overlap also does not contribute to disintegration time. Despite the closer contact between the shell and the tablet core at higher percentages of overlap, the overlap of the outline does not significantly increase tablet stability in terms of disintegration times.

Lastly, the influence of external tablet layers (shell, top, and bottom layers) on the printed tablet disintegration time was examined. Inclusion of the top and bottom layers significantly contributed to the increase in the disintegration time, even though the tablet mass was constant (Fig. 3h). However, this result might be less pronounced at higher infills. External layers composed of closely deposited adjacent filament threads act as a barrier to water entry, leading to longer disintegration. These results are supported by the finding of a much slower dissolution of diltiazem from tablets printed with hydroxypropyl methylcellulose (HPMC) based filament when the top and bottom layers were present (24). In addition, the outer shell with low infill appears to be less resistant to disintegration than the high-infill cores without a shell. The 60 and 80 % infill cores without shell provided a significantly longer disintegration in contrast to the 20 % infill with a shell (Fig. 3i). In the case of PVA, the tablet shell disintegrates quicker than a thicker tablet's core. Therefore, a high infill is more important in the stability and resistance of the tablet to mechanical stress. The obtained results are corroborated by the study by Zheng *et al.* where dissolution of paracetamol tablets printed with HPMC-based filament revealed faster drug release in the case of tablets with 20 % infill and 0.4 mm shell (3 hours) compared to tablets with 80 and 100 % infill and without shell (around 8 and 10 hours) (30).

Design of experiments study

Once initial relations were established, the infill percentage, the infill pattern, the layer height, and the diameter of the nozzle were investigated in a DoE study. In addition

to tablet disintegration time, mass uniformity and disintegration time uniformity were studied to gain a deeper understanding of the printing process and tablet reproducibility. The results of all experiments are summarised in Table II. The results of all responses

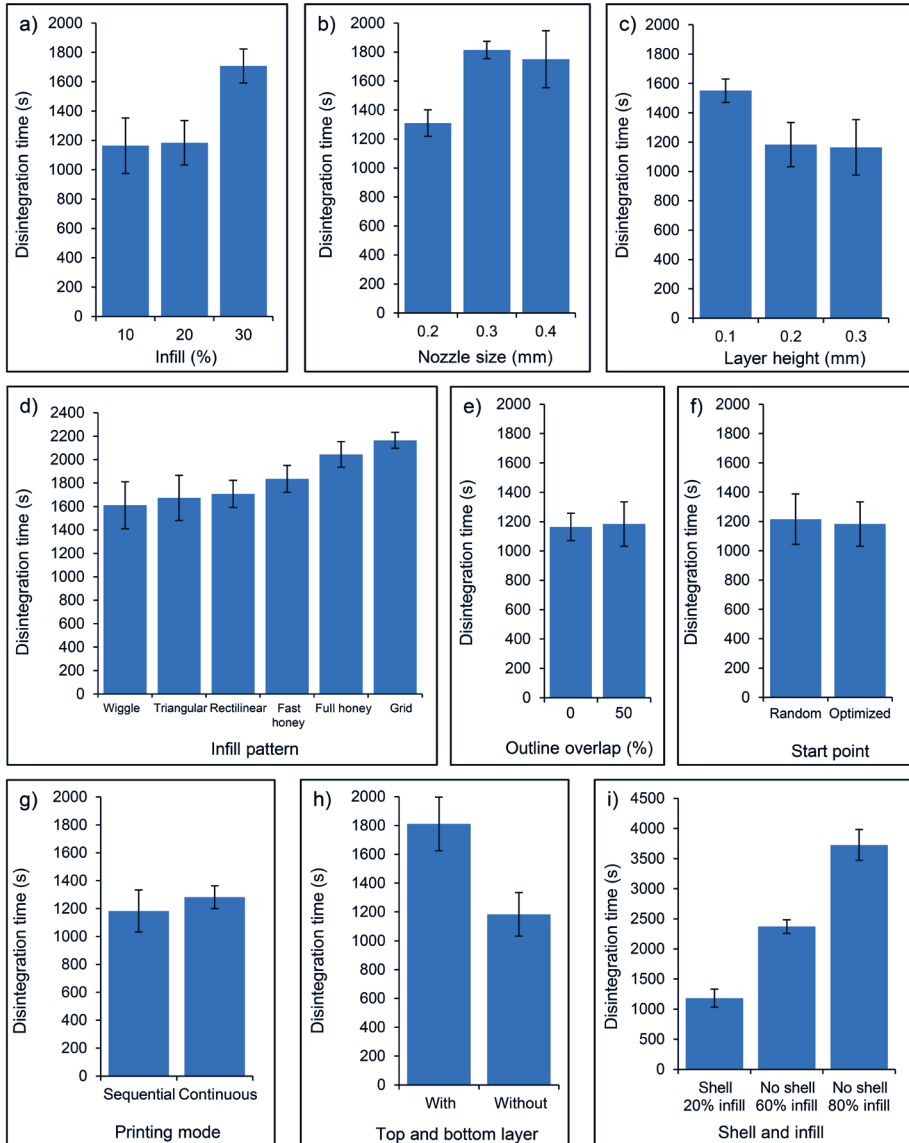


Fig. 3. Influence of process parameters on tablet disintegration time. Influence of: a) infill percentage; b) nozzle size; c) layer height; d) infill pattern; e) outline overlap; f) start point; g) printing mode; h) top and bottom layer presence and i) shell presence.

followed the normal distribution apart from the RSD of the disintegration time, where a logarithmic transformation of the results was used. Well-fitting models with rather good predictability (Q^2 values relatively close to R^2) were obtained (Fig. 4). Variations in tablet disintegration time were well explained by the model ($R^2 = 0.92$). Good models were obtained for the uniformity of mass and the uniformity of disintegration time, which are

Table II. Summary of the results for all the responses in the DoE study

Run	Disintegration time (s)	Disintegration time RSD (%)	Mass RSD (%)
N1	1812	7.98	1.32
N2	2007	10.20	1.36
N3	1454	21.58	1.57
N4	1635	11.69	1.29
N5	2012	11.95	1.19
N6	2141	6.60	1.17
N7	1769	20.08	1.34
N8	2073	8.51	1.30
N9	2358	8.26	0.98
N10	1662	6.69	0.93
N11	2206	4.24	0.93
N12	2092	4.35	0.91
N13	2649	4.71	0.60
N14	1947	7.13	0.81
N15	2070	4.18	1.16
N16	1908	7.86	1.56
N17	2481	4.87	1.38
N18	1836	4.98	1.30
N19	2598	5.88	0.99
N20	2356	8.73	1.12
N21	2481	6.08	1.15
N22	2232	4.36	1.30
N23	2236	2.95	0.94
N24	2357	1.97	1.01
N25	2150	2.09	1.20
N26	1787	5.76	1.16
N27	1948	7.00	0.91
N28	1943	7.87	0.95

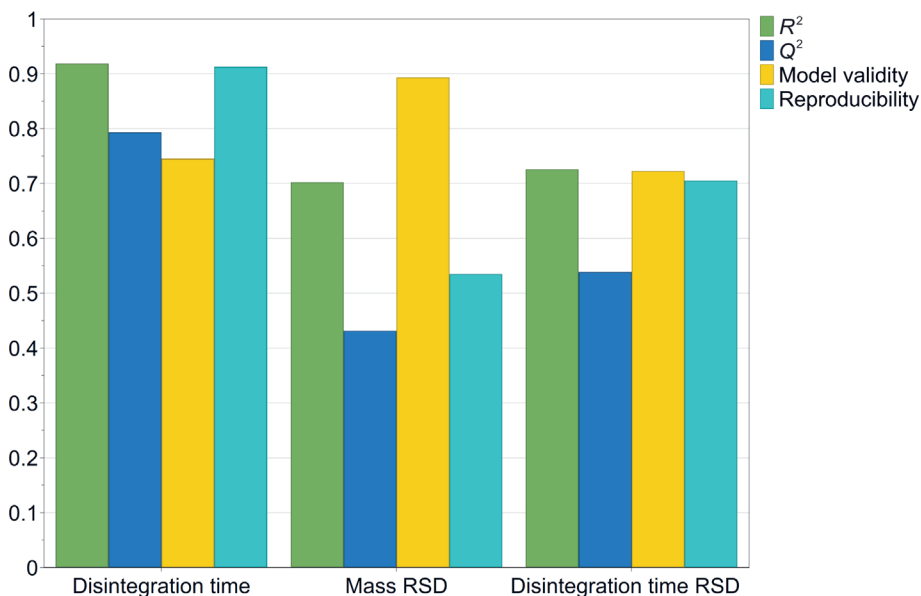


Fig. 4. Summary of fit plot for disintegration time ($R^2 = 0.918$, $Q^2 = 0.793$), uniformity of mass ($R^2 = 0.702$, $Q^2 = 0.432$), and uniformity of disintegration time ($R^2 = 0.726$, $Q^2 = 0.538$).

represented by their relative standard deviations (mass RSD: $R^2 = 0.70$; disintegration time RSD: $R^2 = 0.73$).

The effect of tablet design and printing parameters on the disintegration time was apparent. According to the coefficient plot, the infill percentage, nozzle diameter, and the infill pattern show a significant influence on the disintegration time (Fig. 5a). It was concluded that the infill percentage has the greatest impact on the disintegration time. Not only is the slope on the prediction plot the highest, but the relation is also parabolic (Fig. 6a). The result is in line with several publications on the topic of drug dissolution (3, 28, 31–33). The disintegration time is relatively stable until the infill is set to around 25 %. The percentage of infill could contribute to the disintegration time only after a dense mesh is created. At lower infills, the core of the tablet disintegrates more rapidly than the tablet's shell. This is corroborated in the preliminary study, where no differences in the disintegration time between 10 and 20 % infill were observed. Similarly to the infill percentage, the diameter of the nozzle also significantly affects the disintegration time, but in a linear relationship (Fig. 6b). The nozzle diameter of 0.2 mm leads to disintegration time of around 1900 s, while the diameter of 0.4 mm resulted in disintegration time of around 2100 s. Larger diameters of the nozzles generate thicker filament strands, which slow down the disintegration of the tablet. However, contrary to the finding in the preliminary study, changing the layer height does not appear to have any effect on disintegration time, as regardless of the layer height setting, the disintegration time was comparable at around 2000 s (Fig. 6c). Lastly, different infill patterns affect the disintegration time. The wiggle pattern produced tablets with the fastest disintegration time, while the rectilinear and grid

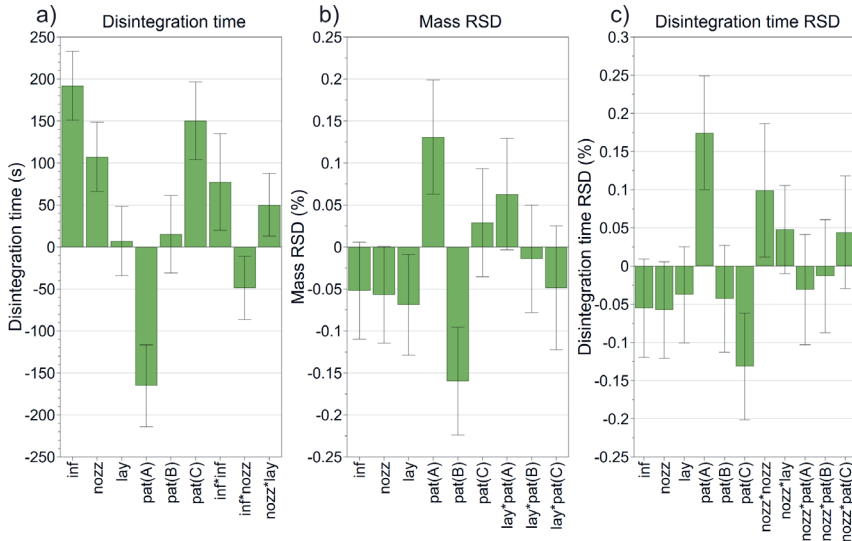


Fig. 5. Coefficient plot of the DoE study, showing the influence of the process parameters and their interactions on: a) the disintegration time; b) mass RSD, and c) disintegration time RSD, where inf is the infill percentage, nozz is the nozzle size, lay is the layer height, pat(A) is the wobble infill pattern, pat(B) is the rectilinear infill pattern, and pat(C) is the grid infill pattern, while an interaction between two parameters is represented by asterisk. If the error bar crosses the line at 0, that parameter is not relevant and does not affect the response significantly.

patterns resulted in moderate and prolonged disintegration times, respectively (Fig. 6d). Tablets with the wobble pattern were especially fragile during handling, as the wobble pattern did not provide support on the short axis. These tablets easily succumbed to squeezing at low forces. Therefore, the selection of an appropriate infill pattern might be the key in extending or facilitating drug dissolution from FDM printed tablets.

Mass uniformity is one of the critical quality parameters for pharmaceutical products. To ensure the correct dose of each individual tablet, the mass variability should be as low as possible. In the printing process, only the layer height and the infill pattern affect the relative standard deviation of the mass (Fig. 5b). The mass uniformity increases with higher layer heights. This can probably be simply explained by the number of material depositions. At lower layer heights, more layers need to be deposited to achieve the same tablet height. An element of error and deposition variability is introduced as more layers are created. Between the infill patterns, the wobble pattern contributed the most to the mass RSD. Despite the fastest disintegration time, it might be the least suitable for the printing process. However, it is worth pointing out that the maximum mass RSD was below 2 % for all experiments. The rectilinear pattern exhibited the lowest inter-tablet mass variation, while the grid pattern resulted in slightly increased mass variation. The uniformity of the disintegration time was also examined. The data were logarithmically transformed to reduce the skewness of the original data. Only the infill pattern impacted the uniformity of the disintegration time (Fig. 5c). The wobble pattern again contributed the most to the RSD of disintegration time, while the grid pattern exhibited the best uniformity in disintegration time.

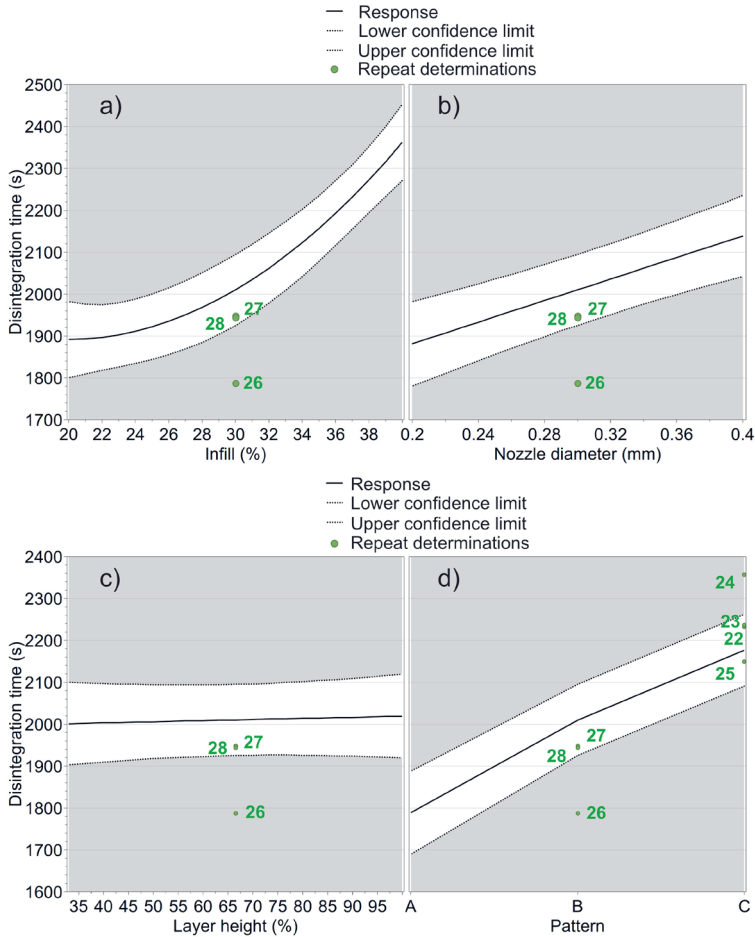


Fig. 6. Prediction plots displaying impact of: a) infill; b) nozzle diameter; c) layer height and d) infill pattern on disintegration time within the input values. Pattern A is wiggle, pattern B is rectilinear, and pattern C is grid infill pattern. The green points represent three repeat measurements of tablets made with the same printing parameters ($n = 3$). Confidence interval was 0.95.

It appears that the infill pattern affects the uniformity of the material deposition and layer fusion. This should be considered when selecting the optimal printing parameters. From a mass uniformity standpoint, the rectilinear infill pattern is the most optimal, while the layer height should be set to high values. However, the infill percentage and nozzle size did not affect either of the RSD values. This shows that the printing process is robust enough to handle wide changes in the dosage form design and process parameters, which is advantageous for the adoption of 3D printing in a pharmaceutical setting.

Two interactions affecting the disintegration time were detected, one between the nozzle diameter and the layer height, and the other between the nozzle diameter and the

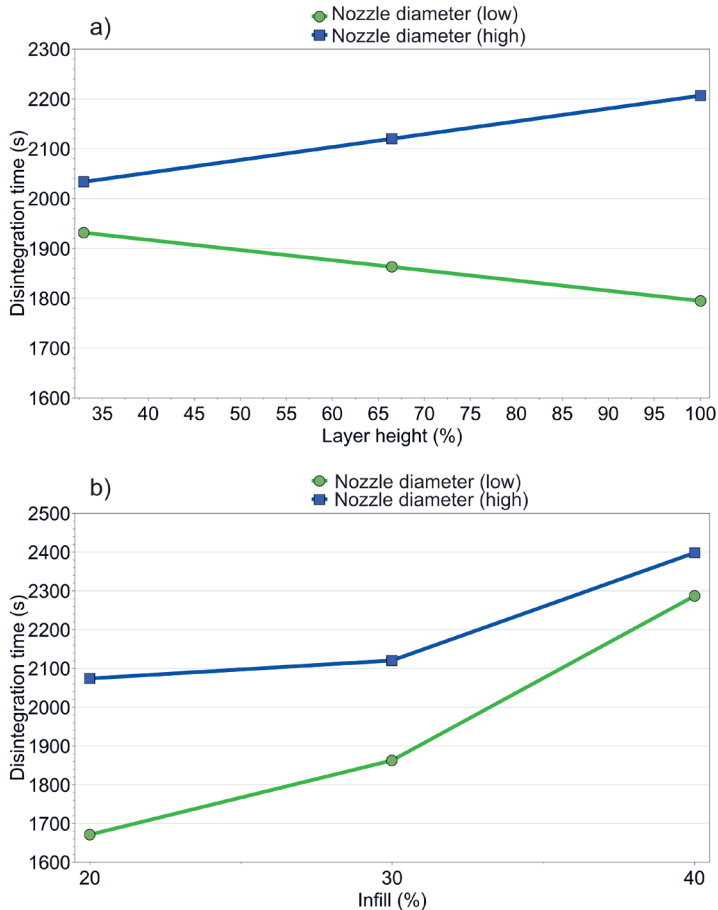


Fig. 7. Interaction plot displaying the effect of varying the nozzle diameter and: a) layer height or the nozzle diameter and b) infill percentage on the tablet disintegration time.

infill percentage (Fig. 7). The first interaction is presumably based on the dimensions of the deposited strands. The width of the deposited strands in the horizontal plane is defined by the diameter of the nozzle, whereas the width in the vertical plane is defined by the layer height. At low layer heights, the filament strands are flat, regardless of their diameter. In such a printing setup, the layers are well fused together because of the high surface contact between the deposited strands. Disintegration times are in such cases comparable regardless of the diameter of the nozzle. However, when the layer height is set to higher values, the nozzle diameter has a greater impact on the disintegration time. In this case, the strands are more upright and can offer less surface area for the interlayer bonds. Thicker strands offer better structural integrity and can lead to slower disintegration times. On the contrary, thin strands disintegrate faster as water ingress is facilitated. This could explain the discrepancy in disintegration times at different nozzle diameter and layer height

settings. The second interaction can be understood as a relation between the density of the tablet core and the thickness of the strand. At low infills, the disintegration time can vary depending on the selected nozzle diameter. It appears that in such instances the tablet core dissolves rapidly, while the shell defines the disintegration time. Larger nozzle diameters and thicker strands could result in slower disintegration of the shell and *vice versa*. Therefore, the nozzle diameter has a greater impact on the disintegration time at lower infill percentages. However, the selection of the nozzle diameter does not appear to affect the disintegration process at high infills. Here, the disintegration time is defined by a densely meshed core. The shell presumably dissolves faster. Regardless of strand thickness, the infill percentage regulates the disintegration time at high values. All in all, the contribution of interactions towards disintegration time is much smaller compared to individual printing parameters.

CONCLUSIONS

The purpose of this study was to better understand the FDM printing process and the uniformity of the prepared tablets. Disintegration time, uniformity of mass, and uniformity of disintegration time were defined as critical quality attributes. Nine process parameters were evaluated in a preliminary study, while four were selected for an in-depth DoE study. The infill percentage and the nozzle size both contributed to the increase in the disintegration time, while their influence on the uniformity of mass and the uniformity of the disintegration time was negligent. The infill pattern proved to be an important parameter for all critical quality attributes investigated. The wobble pattern provided the least amount of internal stability to the tablet core and resulted in the fastest disintegration. It may be less suitable for use in a pharmaceutical setting because of the high mass and disintegration time RSD. The rectilinear pattern slightly prolonged tablet disintegration, while the grid pattern contributed the most to the increase of disintegration time. Both patterns provided excellent uniformity of mass and uniformity of disintegration time. Layer height did not affect disintegration time, but it did influence mass uniformity. It is worth pointing out, that the presented results can only be reproduced by the PVA filament from the same supplier. Commercial filaments normally contain small amounts of various additives to improve the printing process while also altering the properties of the filament. Nevertheless, the general learnings of the article can be applied to other materials and printing scenarios.

Because disintegration and dissolution times are related, our findings could be used to accelerate or prolong drug release with respect to the specific demand. Using FDM, attaining immediate drug release can be challenging due to the inherent slow release of the drug from the polymeric matrix and the lack of appropriate polymers (34). By carefully selecting the tablet design and process parameters, the immediate release profile could be facilitated to a certain extent. The release kinetics of prolonged drug release filaments could also be varied through manipulation of disintegration times.

Slicer software settings have not been thoroughly researched yet. With various options to individually tailor each printed layer, more focus should be put on the field of printing parameters research. In this way, the desired release profiles could be facilitated for an improved personalised therapy.

Funding. – The authors thank Lek Pharmaceuticals d.d. for financial support and material supplied for this study. This research was partly funded by the Slovenian Research Agency under grant number P1-0189. The APC was funded by the Faculty of Pharmacy, University of Ljubljana.

Conflict of interest. – The authors declare that they have no potential conflict of interest.

Authors contributions – Conceptualization, R.D, T.S. and P.P.; methodology, K.K. and T.S.; formal analysis, K.K. and Z.L.; investigation, K.K.; resources, R.D., T.S. and P.P.; original draft preparation, K.K. and Z.L.; review and editing, R.D., T.S. and P.P.; visualization, K.K. and Z.L.; supervision, R.D., T.S. and P.P. All authors have read and agreed to the published version of the manuscript.

REFERENCES

1. A. Samaro, P. Janssens, V. Vanhoorne, J. van Renterghem, M. Eeckhout, L. Cardon, T. de Beer and C. Vervaeke, Screening of pharmaceutical polymers for extrusion-based additive manufacturing of patient-tailored tablets, *Int. J. Pharm.* **586** (2020) 1–11; <https://doi.org/10.1016/j.ijpharm.2020.119591>
2. J. Zhang, X. Feng, H. Patil, R. V. Tiwari and M. A. Repka, Coupling 3D printing with hot-melt extrusion to produce controlled-release tablets, *Int. J. Pharm.* **519**(1-2) (2017) 186–197; <https://doi.org/10.1016/j.ijpharm.2016.12.049>
3. N. G. Solanki, M. Tahsin, A. V. Shah and A. T. M. Serajuddin, Formulation of 3D printed tablet for rapid drug release by fused deposition modeling: Screening polymers for drug release, drug-polymer miscibility and printability, *J. Pharm. Sci.* **107**(1) (2018) 390–401; <https://doi.org/10.1016/j.xphs.2017.10.021>
4. A. Melocchi, F. Parietti, A. Maroni, A. Foppoli, A. Gazzaniga and L. Zema, Hot-melt extruded filaments based on pharmaceutical grade polymers for 3D printing by fused deposition modeling, *Int. J. Pharm.* **509**(1-2) (2016) 255–263; <https://doi.org/10.1016/j.ijpharm.2016.05.036>
5. E. Fuenmayor, M. Forde, A. V. Healy, D. M. Devine, J. G. Lyons, C. McConville and I. Major, Material considerations for fused-filament fabrication of solid dosage forms, *Pharmaceutics* **10**(2) (2018) 1–27; <https://doi.org/10.3390/pharmaceutics10020044>
6. K. Ilyés, N. K. Kovács, A. Balogh, E. Borbás, B. Farkas, T. Casian, G. Marosi, I. Tomuță and Z. K. Nagy, The applicability of pharmaceutical polymeric blends for the fused deposition modelling (FDM) 3D technique: Material considerations–printability–process modulation, with consecutive effects on in vitro release, stability and degradation, *Eur. J. Pharm. Sci.* **129**(1) (2019) 110–123; <https://doi.org/10.1016/j.ejps.2018.12.019>
7. J. Aho, J. P. Bøtker, N. Genina, M. Edinger, L. Arnfast and J. Rantanen, Roadmap to 3D-printed oral pharmaceutical dosage forms: Feedstock filament properties and characterization for fused deposition modeling, *J. Pharm. Sci.* **108**(1) (2019) 26–35; <https://doi.org/10.1016/j.xphs.2018.11.012>
8. C. Korte and J. Quodbach, 3D-printed network structures as controlled-release drug delivery systems: Dose adjustment, API release analysis and prediction, *AAPS PharmSciTech.* **19**(8) (2018) 3333–3342; <https://doi.org/10.1208/s12249-018-1017-0>
9. Q. Li, H. Wen, D. Jia, X. Guan, H. Pan, Y. Yang, S. Yu, Z. Zhu, R. Xiang and W. Pan, Preparation and investigation of controlled-release glipizide novel oral device with three-dimensional printing, *Int. J. Pharm.* **525**(1) (2017) 5–11; <https://doi.org/10.1016/j.ijpharm.2017.03.066>
10. C. I. Gioumouxouzis, A. Baklavariadis, O. L. Katsamenis, C. K. Markopoulou, N. Bouropoulos, D. Tzetzis and D. G. Fatouros, A 3D printed bilayer oral solid dosage form combining metformin for prolonged and glimepiride for immediate drug delivery, *Eur. J. Pharm. Sci.* **120** (2018) 40–52; <https://doi.org/10.1016/j.ejps.2018.04.020>
11. B. Arafat, M. Wojsz, A. Isreb, R. T. Forbes, M. Isreb, W. Ahmed, T. Arafat and M. A. Alhnan, Tablet fragmentation without a disintegrant: A novel design approach for accelerating disintegration and drug release from 3D printed cellulosic tablets, *Eur. J. Pharm. Sci.* **118** (2018) 191–199; <https://doi.org/10.1016/j.ejps.2018.03.019>

12. A. Goyanes, P. Robles Martinez, A. Buanz, A. W. Basit and S. Gaisford, Effect of geometry on drug release from 3D printed tablets, *Int. J. Pharm.* **494**(2) (2015) 657–663; <https://doi.org/10.1016/j.ijpharm.2015.04.069>
13. D. Chen, X. Y. Xu, R. Li, G. A. Zang, Y. Zhang, M. R. Wang, M. F. Xiong, J. R. Xu, T. Wang, H. Fu, Q. Hu, B. Wu, G. R. Yan and T. Y. Fan, Preparation and in vitro evaluation of FDM 3D-printed ellipsoid-shaped gastric floating tablets with low infill percentages, *AAPS PharmSciTech.* **21**(1) (2020) 1–13; <https://doi.org/10.1208/s12249-019-1521-x>
14. F. Baumann, H. Bugdayci, J. Grunert, F. Keller and D. Roller, Influence of slicing tools on quality of 3D printed parts, *Comput. Aided Des. Appl.* **13**(1) (2016) 14–31; <https://doi.org/10.1080/16864360.2015.1059184>
15. T. Feuerbach, S. Kock and M. Thommes, Slicing parameter optimization for 3D printing of bio-degradable drug-eluting tracheal stents, *Pharm. Dev. Technol.* **25**(6) (2020) 650–658; <https://doi.org/10.1080/10837450.2020.1727921>
16. T. Feuerbach, S. Kock and M. Thommes, Characterisation of fused deposition modeling 3D printers for pharmaceutical and medical applications, *Pharm. Dev. Technol.* **23**(10) (2018) 1136–1145; <https://doi.org/10.1080/10837450.2018.1492618>
17. J. Go, S. N. Schiffres, A. G. Stevens and A. J. Hart, Rate limits of additive manufacturing by fused filament fabrication and guidelines for high-throughput system design, *Addit. Manuf.* **16** (2017) 1–11; <https://doi.org/10.1016/j.addma.2017.03.007>
18. R. Jerez-Mesa, G. Gomez-Gras, J. A. Travieso-Rodriguez and V. Garcia-Plana, A comparative study of the thermal behavior of three different 3D printer liquefiers, *Mechatronics* **56** (2018) 297–305; <https://doi.org/10.1016/j.mechatronics.2017.06.008>
19. G. Verstraete, A. Samaro, W. Grymonpré, V. Vanhoorne, B. van Snick, M. N. Boone, T. Hellemans, L. van Hoorebeke, J. P. Remon and C. Vervaet, 3D printing of high drug loaded dosage forms using thermoplastic polyurethanes, *Int. J. Pharm.* **536**(1) (2018) 318–325; <https://doi.org/10.1016/j.ijpharm.2017.12.002>
20. S. Palekar, P. K. Nukala, S. M. Mishra, T. Kipping and K. Patel, Application of 3D printing technology and quality by design approach for development of age-appropriate pediatric formulation of baclofen, *Int. J. Pharm.* **556** (2019) 106–116; <https://doi.org/10.1016/j.ijpharm.2018.11.062>
21. E. Fuenmayor, M. Forde, A. V. Healy, D. M. Devine, J. G. Lyons, C. McConville and I. Major, Comparison of fused-filament fabrication to direct compression and injection molding in the manufacture of oral tablets, *Int. J. Pharm.* **558** (2019) 328–340; <https://doi.org/10.1016/j.ijpharm.2019.01.013>
22. A. Goyanes, F. Fina, A. Martorana, D. Sedough, S. Gaisford and A. W. Basit, Development of modified release 3D printed tablets (printlets) with pharmaceutical excipients using additive manufacturing, *Int. J. Pharm.* **527**(1-2) (2017) 21–30; <https://doi.org/10.1016/j.ijpharm.2017.05.021>
23. Y. Yang, H. Wang, H. Li, Z. Ou and G. Yang, 3D printed tablets with internal scaffold structure using ethyl cellulose to achieve sustained ibuprofen release, *Eur. J. Pharm. Sci.* **115** (2018) 11–18; <https://doi.org/10.1016/j.ejps.2018.01.005>
24. H. Kadry, T. A. Al-Hilal, A. Keshavarz, F. Alam, C. Xu, A. Joy and F. Ahsan, Multi-purposable filaments of HPMC for 3D printing of medications with tailored drug release and timed-absorption, *Int. J. Pharm.* **544**(1) (2018) 285–296; <https://doi.org/10.1016/j.ijpharm.2018.04.010>
25. P. K. Nukala, S. Palekar, N. Solanki, Y. Fu, M. Patki, A. A. Shohatee, L. Trombetta and K. Patel, Investigating the application of FDM 3D printing pattern in preparation of patient-tailored dosage forms, *3D Print. Med.* **3**(1) (2019) 23–37; <https://doi.org/10.2217/3dp-2018-0028>
26. K. Pietrzak, A. Isreb and M. A. Alhnan, A flexible-dose dispenser for immediate and extended release 3D printed tablets, *Eur. J. Pharm. Biopharm.* **96** (2015) 380–387; <https://doi.org/10.1016/j.ejpb.2015.07.027>
27. E. Carlier, S. Marquette, C. Peerboom, L. Denis, S. Benali, J. M. Raquez, K. Amighi and J. Goole, Investigation of the parameters used in fused deposition modeling of poly(lactic acid) to optimize 3D printing sessions, *Int. J. Pharm.* **565** (2019) 367–377; <https://doi.org/10.1016/j.ijpharm.2019.05.008>

28. Y. Joo, I. Shin, G. Ham, S. M. Abuzar, S. M. Hyun and S. J. Hwang, The advent of a novel manufacturing technology in pharmaceuticals: superiority of fused deposition modeling 3D printer, *J. Pharm. Investig.* **50** (2020) 131–145; <https://doi.org/10.1007/s40005-019-00451-1>
29. M. Alhijaj, J. Nasereddin, P. Belton and S. Qi, Impact of processing parameters on the quality of pharmaceutical solid dosage forms produced by fused deposition modeling (FDM), *Pharmaceutics* **11**(12) (2019) 1–21; <https://doi.org/10.3390/pharmaceutics11120633>
30. J. Zhang, W. Yang, A. Q. Vo, X. Feng, X. Ye, D. W. Kim and M. A. Repka, Hydroxypropyl methylcellulose-based controlled release dosage by melt extrusion and 3D printing: Structure and drug release correlation, *Carbohydr. Polym.* **177** (2017) 49–57; <https://doi.org/10.1016/j.carbpol.2017.08.058>
31. M. Tidau, A. Kwade and J. H. Finke, Influence of high, disperse api load on properties along the fused-layer modeling process chain of solid dosage forms, *Pharmaceutics* **11**(4) (2019) 1–17; <https://doi.org/10.3390/pharmaceutics11040194>
32. W. Kempin, V. Domsta, G. Grathoff, I. Brecht, B. Semmling, S. Tillmann, W. Weitschies and A. Seidlitz, Immediate release 3D-printed tablets produced via fused deposition modeling of a thermo-sensitive Drug, *Pharm. Res.* **35**(6) (2018) 1–12; <https://doi.org/10.1007/s11095-018-2405-6>
33. C. Wei, N. G. Solanki, J. M. Vasoya, A. V. Shah and A. T. M. Serajuddin, Development of 3D printed tablets by fused deposition modeling using polyvinyl alcohol as polymeric matrix for rapid drug release, *J. Pharm. Sci.* **109**(4) (2020) 1558–1572; <https://doi.org/10.1016/j.xphs.2020.01.015>
34. D. K. Tan, M. Maniruzzaman and A. Nokhodchi, Advanced pharmaceutical applications of hot-melt extrusion coupled with fused deposition modelling (FDM) 3D printing for personalised drug delivery, *Pharmaceutics* **10**(4) (2018) 1–23; [10.3390/pharmaceutics10040203](https://doi.org/10.3390/pharmaceutics10040203)